

Polarons and bipolarons in Rydberg-dressed extended Bose-Hubbard model

G. A. Domínguez-Castro,¹ L. Santos,¹ and L. A. Peña Ardila^{2,3}

¹*Institut für Theoretische Physik, Leibniz Universität Hannover, Appelstrasse 2, D-30167 Hannover, Germany*

²*School of Science and Technology, Physics Divisio, University of Camerino,
Via Madonna delle Carceri, 9B - 62032 (MC), Italy*

³*Dipartimento di Fisica, Università di Trieste, Strada Costiera 11, I-34151 Trieste, Italy**

(Dated: November 12, 2024)

Impurities immersed in hard-core Bose gases offer exciting opportunities to explore polaron and bipolaron physics. We investigate the ground state properties of a single and a pair of impurities throughout the superfluid and insulating (charge density wave) phases of the bosonic environment. In the superfluid phase, we demonstrate that the impurity undergoes a polaron-like transition, shifting from behaving as an individual particle to becoming a dressed quasiparticle as the coupling with the bath increases. However, in the insulating phase, the impurity can maintain its individual character, moving through a potential landscape shaped by the charge density wave order. Moreover, we show that two impurities can form a bound state even in the absence of an explicit impurity-impurity coupling. Furthermore, we establish the stability of this bound state within both the superfluid and insulating phases. Our results offer valuable insights for ongoing lattice polaron experiments with ultracold gases.

I. INTRODUCTION

Polarons arising from the interaction between mobile impurities and their host environment have provided valuable insights into quantum many-body systems [1, 2], offering simple yet accurate descriptions of a wide range of physical systems, including liquid helium mixtures [3, 4], ultracold atomic gases [5–9], doped antiferromagnets [10, 11], and hybrid light-matter materials [12, 13], among others. On the other hand, ultracold atoms in optical lattices provide a powerful quantum simulation platform for strongly correlated phenomena [14, 15], interestingly due to the translational breaking of symmetry, new phases arise when optical lattices are doped as the size of the polaron can be comparable with the lattice size [16–20]. This includes the behavior of strongly interacting polarons in environments undergoing quantum phase transitions [21–23], impurity dynamics [24–29], the formation of bipolarons [30–40], polarons in topological media [41–45], and the intricate interplay between kinetic energy and spin interactions in doped Mott insulators [46–48].

Recently, the one-dimensional extended Bose-Hubbard model (eBHM) with nearest-neighbor interactions was successfully realized using Rydberg-dressed atoms [49]. Furthermore, the eBHM with longer-range interactions was implemented using magnetic atoms [50] and could potentially be realized with polar molecules in the upcoming generation experiments [51, 52]. These breakthrough experiments open up exciting new avenues for exploring impurity physics within an itinerant, long-range interacting quantum gas. Moreover, the eBHM exhibits a superfluid-to-insulator phase transition [53, 54], making it an appealing environment for studying the be-

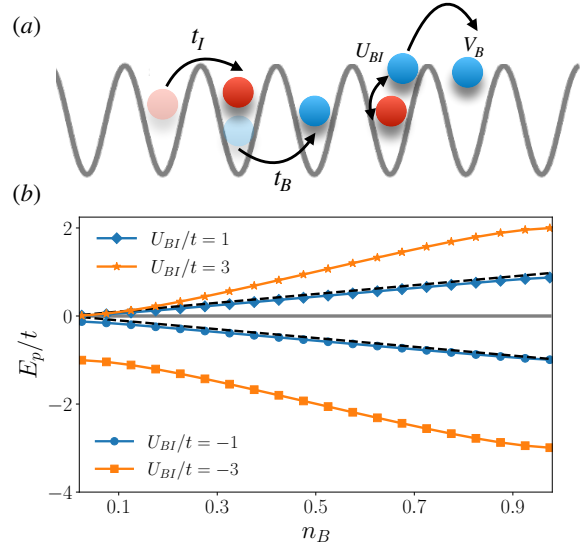


FIG. 1. (a) Illustration of the system considered. Mobile impurities (red spheres) immersed in an interacting hard-core Bose gas (blue spheres) in a one-dimensional optical lattice. The tunneling amplitude for bosons and impurities are denoted by t_B and t_I , respectively. The interaction among bosons is represented by V_B , while the boson-impurity interaction is denoted by U_{BI} . (b) Binding energy E_p of a single impurity as a function of the density of the bath n_B . Markers are associated with DMRG calculations, whereas the dashed lines correspond to the mean-field prediction $E_p \approx U_{BI}n_B$. The gray line represents a guide for the eye for zero energy. We consider $V_B/t = 0$.

havior of impurities across this transition. Understanding the underlying physics of impurities in insulating media has gained increasing relevance [55, 56], particularly in light of recent semiconductor experiments [57–59].

In this work, we study the quasiparticle properties of a single and a pair of impurities immersed in an interacting

* luisaldemar.penaardila@units.it

hard-core Bose gas on a one-dimensional lattice. Such a system can be realized by doping with impurities the Rydberg-dressed gas in Ref. [49]. Using density matrix renormalization group (DMRG) techniques, we first describe the ground-state properties of an impurity across the superfluid (SF) and charge density wave (CDW) phases of the bosonic medium. In contrast to the superfluid phase, where the impurity transitions from behaving as an individual particle to a dressed object as its coupling with the environment increases, in the CDW phase, the impurity retains its single-particle character but moves in a potential landscape shaped by the CDW order, which can be effectively described by an ionic Hubbard model [60–64] (IHM). For the case of two impurities, we numerically demonstrate that the impurities can form a bound state even in the absence of an explicit impurity-impurity coupling, and we establish the stability of this bound state within both the SF and CDW phases.

This manuscript is organized as follows. We introduce the model under study in Sec. II. In Sec. III, we examine the binding energy, quasiparticle residue, and resulting spatial bath-impurity correlations for a single impurity. Section IV addresses the two-impurity problem, with a particular focus on bipolaron state formation. Finally, in Sec. V, we summarize our findings.

II. MODEL

We consider mobile impurities doping interacting hard-core bosons in a one-dimensional lattice, see Fig. 1(a). The Hamiltonian of the system can be written as $\hat{H} = \hat{H}_B + \hat{H}_I + \hat{H}_{BI}$, where \hat{H}_B describes the bosonic bath, \hat{H}_I the impurities, and \hat{H}_{BI} denotes the coupling between the bath and the impurities. Explicitly, each component is given as follows:

$$\begin{aligned} \hat{H}_B &= -t_B \sum_{\langle i,j \rangle} \hat{b}_i^\dagger \hat{b}_j + V_B \sum_i \hat{n}_{B,i} \hat{n}_{B,i+1} \\ \hat{H}_I &= -t_I \sum_{\langle i,j \rangle} \hat{a}_i^\dagger \hat{a}_j \quad \hat{H}_{BI} = U_{BI} \sum_i \hat{n}_{I,i} \hat{n}_{B,i}, \end{aligned} \quad (1)$$

where operators \hat{b}_i^\dagger (\hat{b}_i) and \hat{a}_i^\dagger (\hat{a}_i) create (annihilate) a boson and an impurity, respectively, at lattice site i . The particle number operator for the bosons is $\hat{n}_{B,i} = \hat{b}_i^\dagger \hat{b}_i$, and for the impurities $\hat{n}_{I,i} = \hat{a}_i^\dagger \hat{a}_i$. The nearest neighbor hopping amplitude is t_B and t_I for the bosons and impurities, respectively; $V_B > 0$ is the nearest-neighbor repulsive interaction among the particles in the bath, and U_{BI} is the on-site interaction between the bosons and the impurities. The hard-core constraint of the bath atoms forbids double occupancy, i.e. $(\hat{b}_i^\dagger)^2 = 0$. This restriction can be experimentally achieved using sufficiently strong on-site interactions [49]. We do not impose the hard-core constraint on the impurities. Notice that \hat{H}_I does not explicitly include an impurity-impurity interaction term.

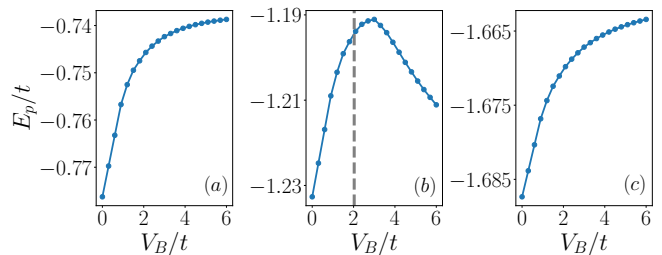


FIG. 2. (a)-(c) Binding energy E_p of a single impurity as a function of the boson-boson interaction V_B/t for $n_B = 0.25, 0.5$ and 0.75 , respectively. The grey dashed line indicates the value of V_B/t at which the SF-CDW transition takes place. We consider $U_{BI}/t = -2$.

To investigate the ground state properties of a single and a pair of impurities, we employ density matrix renormalization group (DMRG) techniques using the TeNPy library [65]. All calculations assume periodic boundary conditions on a lattice with $L = 80$ sites and a maximum matrix product state (MPS) bond dimension of $\chi = 800$. For concreteness, we consider the case where $t_B = t_I = t$.

III. SINGLE IMPURITY

Before delving into the study of impurities, it is instructive to briefly review the ground-state properties of the bosonic medium in the absence of impurities. For repulsive inter-site interactions $V_B > 0$, the hard-core bosons exhibit either a superfluid or an insulating charge density wave phase. The latter occurs exclusively at half filling $n_B = 1/2$ and $V_B/t > 2$ [66]. The SF phase is a gapless phase with power-law decaying one-body correlation functions. In contrast, the CDW is a gapped phase marked by exponentially decaying one-body correlation functions. In the atomic limit $t = 0$, the charge density wave acquires the simple form $|\cdots \bullet \circ \bullet \circ \bullet \circ \cdots\rangle$ (where \bullet and \circ denote an occupied and empty site, respectively).

We begin the single impurity analysis by computing the binding energy E_p of the impurity. Physically, E_p corresponds to the energy required to add a single impurity into the medium. The binding energy can be computed as follows

$$E_p = E_1 - (E_0 + E_I), \quad (2)$$

where E_0 and E_1 denote the ground-state energies of the system with zero and one impurity, respectively, and E_I represents the energy of a single free impurity. As a result of the lattice dispersion $E_I/t = -2$.

In Fig. 1(b), we show the binding energy of the impurity as a function of the medium density for several values of the bath-impurity interaction and fixed $V_B/t = 0$. As observed, for small boson-impurity interactions ($U_{BI} \lesssim t$), E_p follows the mean-field predictions, $E_p \approx U_{BI} n_B$. However, stronger boson-impurity

interactions reveal non-linear density behavior, highlighting the relevance of beyond mean-field terms. In the limit of a sparse bosonic bath and attractive interactions $U_{BI} < 0$, E_p converges to the binding energy of the boson-impurity bound state. Note that this is not the case for $U_{BI} > 0$, as the repulsively bound pair is not the two-body ground state. Similar conclusions are drawn in two-dimensional systems, where beyond-Fröhlich terms account for the non-zero value of E_p in the attractive branch [67]. Figs. 2(a)-2(c) illustrates E_p as a function of V_B for three different bosonic fillings and $U_{BI}/t = -2$. For $n_B = 0.25$ and $n_B = 0.75$, E_p increases as the bosons become strongly interacting. At half-filling, the binding energy bends around the superfluid-insulator transition, suggesting a change in the behavior of the impurity across the second-order phase transition of the medium.

To study the spectral features of the impurity, we compute its quasiparticle residue Z . This quantity measures the spectral weight of the quasiparticle and quantifies how particle-like impurity behaves in an interacting medium. The residue is defined as the square of the overlap between the interacting ground state and the non-interacting boson-impurity state

$$Z = |\langle \Psi_1(n_B, V_B, U_{BI}) | \Psi_1(n_B, V_B, 0) \rangle|^2, \quad (3)$$

where $\Psi_1(n_B, V_B, U_{BI})$ denotes the ground state of the environment with one impurity for the system parameters (n_B, V_B, U_{BI}) . In Figs. 3(a)-3(d), we show the value of Z as a function of U_{BI}/t for different values of n_B and V_B/t . We observe that for $0 < n_B < 1/2$, the attractive polaron is more robust, as the repulsive polaron loses its spectral weight more rapidly with increasing boson-impurity interaction. Due to particle-hole symmetry, the opposite is true for $n_B > 1/2$ (see Appendix A).

As the interaction among the bosons of the bath becomes stronger, the residue around $n_B = 1/2$ increases, indicating that the impurity resumes its individual particle character. This occurs because the CDW phase exhibits a gap of the order $\propto V_B$, and small enough boson-impurity interactions do not significantly alter the CDW background. Consequently, the impurity moves on top of this static background, which behaves as an external potential. To illustrate the latter, let us consider the deep insulating regime of the bath, where density fluctuations can be neglected. In this scenario, one can approximate the bosonic operators by their expectation values $\langle \hat{b}_i \rangle \approx 0$ and $\langle \hat{n}_{B,i} \rangle \approx 1/2$. This approach is equivalent to considering the zero particle-hole excitations subspace of the CDW [56], and one can use an effective single-particle Hamiltonian for the impurity,

$$\hat{H}_I^{\text{eff}} = -t \sum_{\langle i,j \rangle} \hat{a}_i^\dagger \hat{a}_j + \frac{U_{BI}}{2} \sum_i (-1)^i \hat{n}_{I,i}, \quad (4)$$

where the boson-impurity coupling becomes an alternating local potential. The Hamiltonian in Eq. (4) takes the form of the celebrated ionic Hubbard model [60–64].

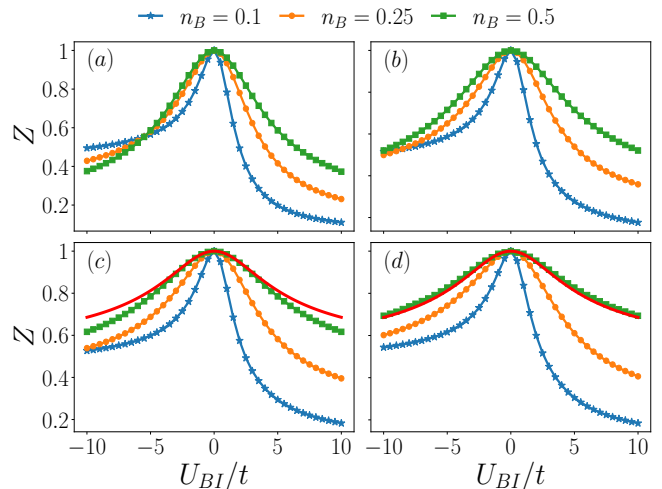


FIG. 3. Quasiparticle residue Z as a function of the boson-impurity interaction U_{BI}/t . Panels (a), (b), (c), and (d) are associated with $V_B/t = 0, 1, 2$, and 6 , respectively. The red line in panels (c) and (d) corresponds to the overlap between the unmodulated and modulated single-particle ground states of the ionic Hubbard model.

This model has been employed to describe the neutral-ionic transition in quasi-one-dimensional charge-transfer organic materials [68–71], and the ferroelectric transitions in perovskites [72, 73]. In our system, the potential modulation emerges as a consequence of the formation of the CDW and the boson-impurity coupling. As depicted in Fig. 3(c) and Fig. 3(d), the square of the overlap between the unmodulated ($U_{BI}/t = 0$) and modulated ($U_{BI}/t \neq 0$) single-particle ground states of Hamiltonian in Eq. (4) agrees with DMRG calculations for $n_B = 1/2$, proving the accuracy of the effective Hamiltonian.

To conclude the single impurity section, we analyze the density-density impurity-boson correlation function defined as

$$\mathcal{C}_{BI}(|i-j|) = L[\langle \hat{n}_{B,i} \hat{n}_{I,j} \rangle - \langle \hat{n}_{B,i} \rangle \langle \hat{n}_{I,j} \rangle], \quad (5)$$

this observable $\mathcal{C}_{BI}(|i-j|)$ gives the deviation from the background value of the number of bosons at site i given that the impurity is at site j . Quantum gas microscopy and quench protocols [74] can be used to obtain information on the above correlator. For simplicity, we consider the case $U_{BI}/t < 0$, and the results associated with $U_{BI}/t > 0$ can be found in the Appendix A. Figure 4(a) shows $\mathcal{C}_{BI}(0)$ as a function of U_{BI}/t for several values of n_B , we consider a noninteracting medium $V_B = 0$. As expected, the dressing on top of the impurity raises as U_{BI}/t becomes more attractive, initially displaying a linear increase for small values of U_{BI}/t , consistent with a perturbative approach, before saturating at strong boson-impurity interactions. Interestingly, we find that $\mathcal{C}_{BI}(0)$ decreases as the bosonic medium becomes denser. However, as illustrated in Fig. 4(b), the dressing cloud becomes more spatially extended in a denser bosonic en-

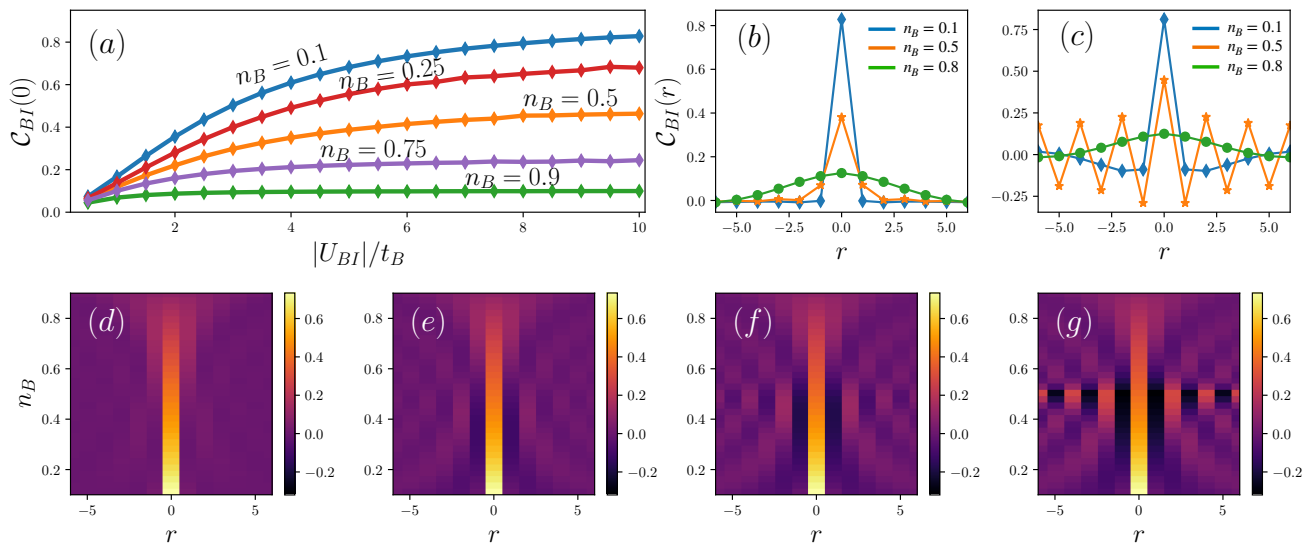


FIG. 4. (a) Density-density boson-impurity correlation $\mathcal{C}_{BI}(r)$ at the same site ($r = 0$) as a function of the interaction U_{BI}/t for several bosonic filling factors n_B and fixed $V_B = 0$. (b) $\mathcal{C}_{BI}(r)$ as a function of the relative distance r for three different values of n_B and $(V_B/t, U_{BI}/t) = (0, -10)$. (c) Same as panel (b) but for $(V_B/t, U_{BI}/t) = (4, -10)$. (d)-(g) Development of the density-density boson-impurity correlations as the medium transitions from the superfluid to the charge density wave for $U_{BI}/t = -6$. Panels (d), (e), (f) and (g) are associated with $V_B/t = 0, 1, 2$, and 4 respectively.

vironment.

As the bath becomes strongly interacting, the behavior of the boson-impurity correlations changes significantly. Fig. 4(c) shows that the impurity repels the bosons from its nearest neighboring sites, contrasting sharply with the non-interacting case, where only positive correlations are observed. In the half-filled scenario, the impurity inherits the CDW correlations since for large U_{BI} , it can bind a boson with an impurity. Figs. 4(d)-4(g) display in a color scheme the development of the boson-impurity correlations \mathcal{C}_{BI} as the medium transitions from the superfluid to the CDW, we consider $U_{BI}/t = -6$. The impurity provides an unambiguous quantum probe of the emerging CDW correlations.

IV. TWO IMPURITIES

We analyze at this point the case of two impurities immersed in the interacting hard-core Bose gas. We focus on the repulsive branch $U_{BI} > 0$ only. Despite the absence of an explicit impurity-impurity interaction term, strong density fluctuations of the bosonic bath surrounding an impurity can induce an effective interaction with a nearby impurity [33, 37, 75, 76]. This interaction can be strong enough to bind two impurities, giving rise to the formation of a bipolaron. Analogously to the previous section, we first focus on the binding energy, for the case of two impurities, the binding energy E_{Bip} is defined as follows

$$E_{Bip} = E_2 - 2E_1 + E_0, \quad (6)$$

where E_2 is the ground-state energy of the bosonic medium with two impurities and as before E_1 and E_0 denote the energy with one and zero impurities, respectively. Figures 5(a)-5(d) illustrate E_{Bip} as a function of the boson-impurity interaction for several values of the bosonic filling and the boson-boson interaction. In the SF regime (Figs. 5(a)-5(b)) and $U_{BI}/t \gtrsim 1.8$, the binding energy becomes clearly negative, signaling the formation of a bound state. Interestingly, the binding energy displays an essentially density-independent behavior for small boson-impurity couplings, while larger values of U_{BI}/t reveal that the impurities bind more tightly as the medium is more compressible [75].

As the bath becomes strongly interacting, density fluctuations decrease, hindering the formation of the bound state close to half-filling. This is clearly illustrated in Figs. 5(b)-5(d), where E_{Bip} is pushed towards zero for half-filled (and close to half-filled) bosonic media. However, the bound state emerges for $U_{BI} \gtrsim V_B$. Physically, this behavior can be understood by noting that the CDW exhibits a gap of the order $\propto V_B$, boson-impurity interactions of this magnitude promote density fluctuations in the medium, thereby enhancing the induced impurity-impurity interaction. Notably, the binding energy associated with low bath densities remains largely unaffected by the interaction between the bosons. In contrast to Figs. 5(a) and 5(b) the impurities bind more tightly for medium densities away from half-filling. We have checked that when considering hard-core impurities, the binding energy is always positive (see Appendix B), showing the crucial role played by the quantum statistics of the impurities.

To further characterize the bound state formation, we

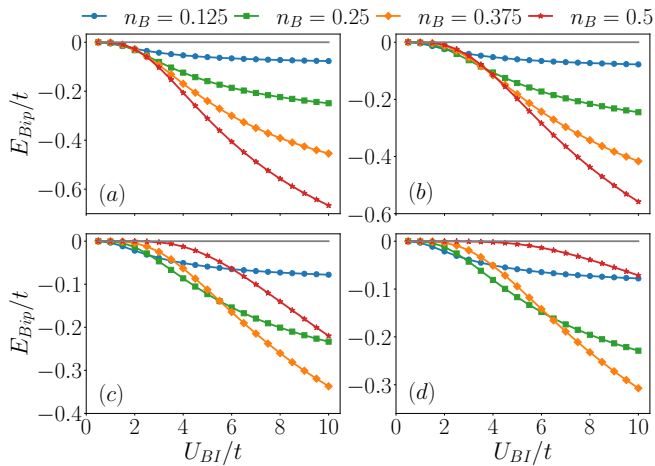


FIG. 5. Binding energy E_{BIP} of the two-impurity state as a function of the boson-impurity interaction U_{BI}/t for several values of the bosonic filling n_B . Panels (a), (b), (c) and (d) consider $V_B/t = 0, 1, 3$ and 4 , respectively. The gray line represents a guide for the eye for zero energy.

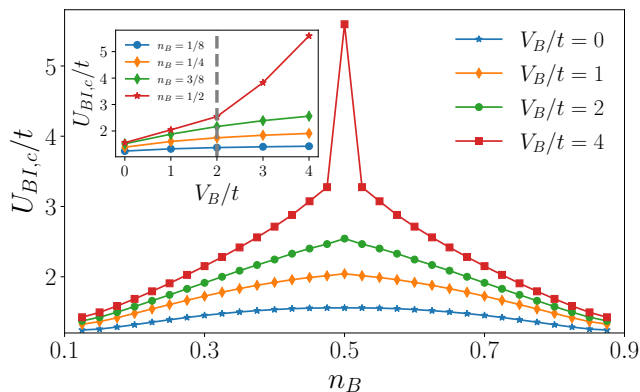


FIG. 6. Critical boson-impurity interaction $U_{BI,c}$ at which $E_B/t = -\delta$ as a function of the medium density for several values of the boson-boson interaction V_B . Inset shows $U_{BI,c}$ as a function of the boson-boson interaction for several values of medium density. The grey dashed line indicates the value of V_B/t at which the SF-CDW transition takes place. We consider $\delta = 0.01$.

define the critical boson-impurity interaction $U_{BI,c}$ as the value for which the binding energy is equal to a given threshold, i.e., $E_B(U_{BI,c})/t = -\delta$. Fig. 6 displays $U_{BI,c}$ as a function of the bosonic density n_B for several values of V_B . We consider $\delta = 0.01$, but other reasonably small values of δ do not significantly alter the results. The suppression of the density fluctuations as V_B increases gives rise to an increase of $U_{BI,c}$. The inset of Fig. 6 illustrates $U_{BI,c}$ as a function of V_B for several values of n_B , one can notice the abrupt change on $U_{BI,c}$ once the medium enters a gapped phase.

Signatures of bound state formation can also be obtained by the impurity-impurity correlation function

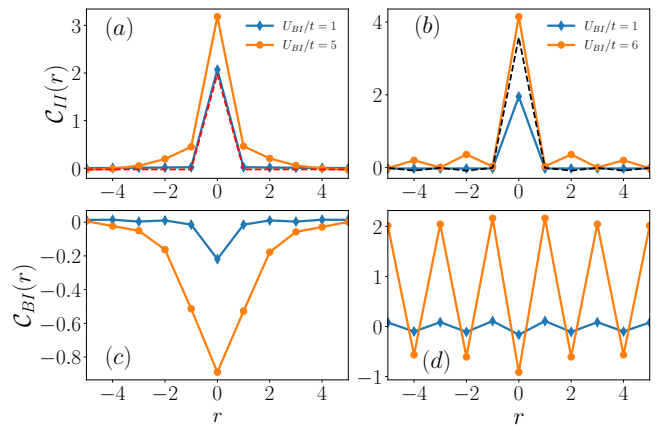


FIG. 7. (a) Impurity-impurity correlation $\mathcal{C}_{II}(r)$ as a function of the distance r for $(n_B, V_B/t) = (0.375, 0)$, dashed line corresponds to the impurity-impurity correlation for two free impurities in the absence of the bosonic environment. (b) same as (a), but for $(n_B, V_B/t) = (0.5, 4)$, the dashed line is associated with the impurity-impurity correlation for two free impurities in the IHM. (c) Boson-impurity correlation $\mathcal{C}_{BI}(r)$ as a function of the relative distance r for $(n_B, V_B/t) = (0.375, 0)$. (d) same as (c) but we consider $(n_B, V_B/t) = (0.5, 4)$.

$\mathcal{C}_{II}(|i-j|) = L[\langle \hat{n}_{I,j} \hat{n}_{I,i} \rangle - \langle \hat{n}_{I,j} \rangle \langle \hat{n}_{I,i} \rangle]$. As depicted in Fig. 7(a) when there is no bound state $(V_B/t, U_{BI}/t) = (0, 1)$, $\mathcal{C}_{II}(r)$ matches the impurity-impurity correlation function associated with two free impurities in the absence of bosonic environment (red dashed line). In contrast, for $(V_B/t, U_{BI}/t) = (0, 5)$, the range of $\mathcal{C}_{II}(r)$ increases as a result of the bound state formation. This indicates that the intrinsic correlations developed as U_{BI} increases are not captured by a free model, emphasizing the crucial role of the environment. Fig. 7(b) illustrates \mathcal{C}_{II} within the CDW phase $V_B/t = 4$, weak boson-impurity interactions lead to similar behavior as in the superfluid phase. In contrast, once the bound state is formed \mathcal{C}_{II} displays modulated correlations with a decreasing envelope. To show that the emerging correlations are due to the mediated interactions and not of the ionic Hubbard model, we plot the impurity-impurity correlation function for two free impurities in the IHM (black dashed line). Alternatively to \mathcal{C}_{II} one can monitor the boson-impurity correlation \mathcal{C}_{BI} . As depicted in Fig. 7(c), within the superfluid phase, the bound state formation is manifested as a large depletion of the local density of the bath. In contrast, within the insulating phase, \mathcal{C}_{BI} inherits an out-of-phase CDW modulation due to the repulsive boson-impurity interaction.

V. CONCLUSIONS

Motivated by recent experimental advances with Rydberg-dressed gases in optical lattices [49], we consider a single and a pair of mobile impurities immersed in an interacting hard-core Bose gas in a one-dimensional lat-

tice. In particular, we investigate how the ground state properties of the impurities change when the environment is in a superfluid or insulating charge density wave phase. Within the superfluid phase, we numerically demonstrate that a single impurity transitions from behaving as an individual particle to a dressed object as its coupling with the environment increases. However, in the insulating phase, the impurity can retain its single-particle character, moving in a potential landscape shaped by the charge density wave order, which can be effectively described by an ionic Hubbard model. For the case of two impurities, we show the formation of a bound state even in the absence of an explicit impurity-impurity interaction. Furthermore, we establish the stability of the bound state, showing its persistence when the environment enters the strongly interacting regime. In addition, we illustrate that experimentally relevant density-density correlations can also offer clear signatures of bound state formation. The discussed results provide valuable insights for ongoing lattice polaron experiments with ultracold gases in low-dimensional systems.

ACKNOWLEDGMENTS

We thank Arturo Camacho-Guardian and Thomás Fogarty for their valuable comments on our manuscript. L.S. and G.A.D.-C. acknowledge support of the Deutsche Forschungsgemeinschaft (DFG, German Research Foundation) under Germany's Excellence Strategy, EXC-2123 QuantumFrontiers, Grant No. 390837967 and LAPA acknowledges financial support from PNRR MUR project PE0000023-NQSTI.

Appendix A: Single impurity

In this section, we provide extended results for the case of a single impurity. Due to the particle-hole symmetry $n_B \rightarrow 1 - n_B$ of H_B , the Hamiltonian associated with the bath, the quasiparticle residue of the impurity inherits a symmetry under $(n_B, U_{BI}) \rightarrow (1 - n_B, -U_{BI})$. To show this behavior, in Fig. 8 we plot Z as a function of the boson-impurity interaction U_{BI}/t . In contrast to Fig. 3, for $n_B > 1/2$ the residue of the attractive polaron quickly decays when U_{BI}/t becomes more negative and the repulsive polaron stands as a more robust quasiparticle.

To end this section, we present extended results of the boson-impurity correlations for $U_{BI}/t > 0$. In contrast to Fig. 4, for $U_{BI}/t > 0$ density fluctuations of the bosonic medium increase as the n_B increases. Figs. 10(d)-10(g) display in a color scheme the change of $\mathcal{C}_{BI}(r)$ as the medium transitions from the superfluid to the charge density wave phase, we consider $U_{BI}/t = 6$. As for the attractive case, the impurity provides an unambiguous probe of the emerging correlations of the medium as it enters the CDW phase.

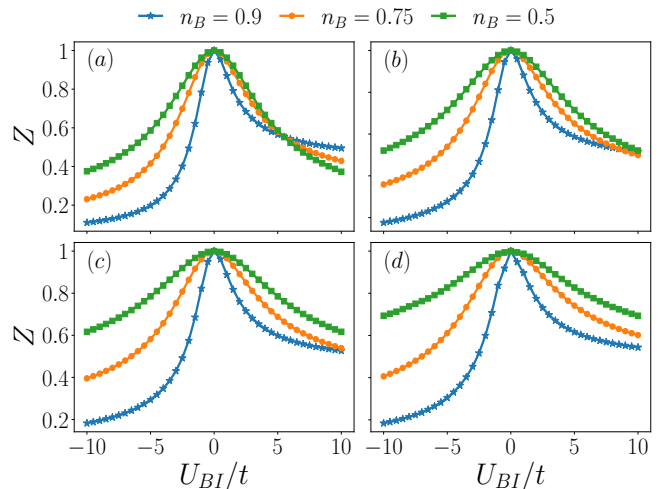


FIG. 8. Quasiparticle residue Z as a function of the boson-impurity interaction U_{BI}/t for three different values of the bosonic filling n_B . Panels (a)-(d) are associated with $V_B/t = 0, 1, 2,$ and 6 , respectively.

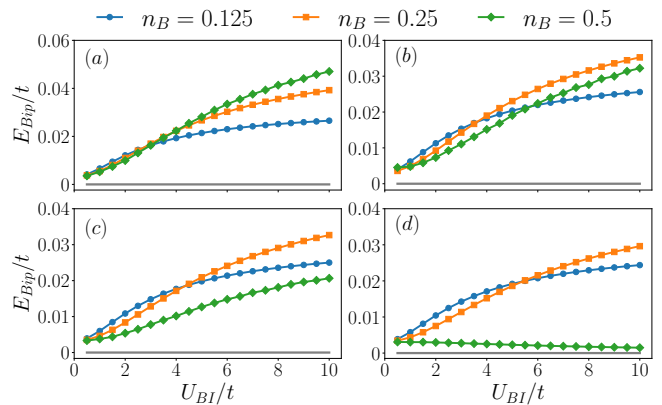


FIG. 9. Binding energy E_{Bip} of two hard-core impurities as a function of the boson-impurity interaction U_{BI}/t for several values of the bosonic filling n_B . Panels (a), (b), (c), and (d) consider $V_B/t = 0, 1, 2,$ and 3 , respectively. The gray line represents a guide for the eye for zero energy.

Appendix B: Two impurities

In the following, we provide extended results associated with the case of two impurities. In Fig. 9, we plot the binding energy of two hard-core impurities. In stark contrast to soft-core impurities, E_{Bip} is not negative in the range of U_{BI}/t investigated. Consequently, there is no formation of a bound state, regardless of the density of the bosonic bath.

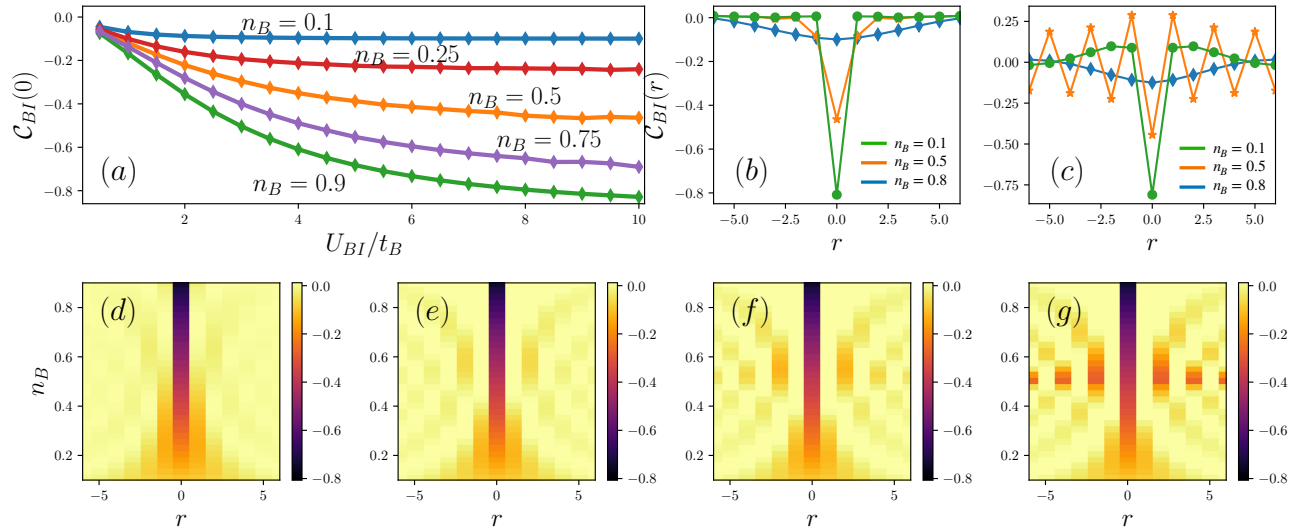


FIG. 10. (a) Density-density boson-impurity correlation $\mathcal{C}_{BI}(r)$ at the same site ($r = 0$) as a function of the interaction U_{BI}/t_B for several bosonic filling factors n_B and fixed $V_B = 0$. (b) $\mathcal{C}_{BI}(r)$ as a function of the relative distance r for three different values of n_B and $(V_B/t, U_{BI}/t) = (0, -10)$. (c) Same as panel (b) but for $(V_B/t, U_{BI}/t) = (4, -10)$. (d)-(g) Development of the density-density boson-impurity correlations as the medium transitions from the superfluid to the charge density wave for $U_{BI}/t = 6$. Panels (d), (e), (f), and (g) are associated with $V_B/t = 0, 1, 2$ and 4 , respectively.

-
- [1] L. Landau and S. Pekar, Effective mass of a polaron, *Zh. Eksp. Teor. Fiz* **18**, 419 (1948).
- [2] S. Pekar, Theory of electromagnetic waves in a crystal with excitons, *Journal of Physics and Chemistry of Solids* **5**, 11 (1958).
- [3] G. Baym and C. Pethick, *Landau Fermi-liquid theory: concepts and applications* (John Wiley & Sons, 2008).
- [4] J. Bardeen, G. Baym, and D. Pines, Effective interaction of he^3 atoms in dilute solutions of he^3 in he^4 at low temperatures, *Phys. Rev.* **156**, 207 (1967).
- [5] F. Scazza, M. Zaccanti, P. Massignan, M. M. Parish, and J. Levinsen, Repulsive fermi and bose polarons in quantum gases, *Atoms* **10**, 55 (2022).
- [6] P. Massignan, M. Zaccanti, and G. M. Bruun, Polarons, dressed molecules and itinerant ferromagnetism in ultracold fermi gases, *Reports on Progress in Physics* **77**, 034401 (2014).
- [7] F. Chevy and C. Mora, Ultra-cold polarized fermi gases, *Reports on Progress in Physics* **73**, 112401 (2010).
- [8] R. Schmidt, M. Knap, D. A. Ivanov, J.-S. You, M. Cetina, and E. Demler, Universal many-body response of heavy impurities coupled to a fermi sea: a review of recent progress, *Reports on Progress in Physics* **81**, 024401 (2018).
- [9] F. Grusdt, N. Mostaan, E. Demler, and L. A. Peña Ardila, Impurities and polarons in bosonic quantum gases: a review on recent progress, *arXiv e-prints*, arXiv:2410.09413 (2024), arXiv:2410.09413 [cond-mat.quant-gas].
- [10] E. Dagotto, A. Moreo, and T. Barnes, Hubbard model with one hole: Ground-state properties, *Phys. Rev. B* **40**, 6721 (1989).
- [11] C. L. Kane, P. A. Lee, and N. Read, Motion of a single hole in a quantum antiferromagnet, *Phys. Rev. B* **39**, 6880 (1989).
- [12] M. Sidler, P. Back, O. Cotlet, A. Srivastava, T. Fink, M. Kroner, E. Demler, and A. Imamoglu, Fermi polaron-polaritons in charge-tunable atomically thin semiconductors, *Nature Physics* **13**, 255 (2017).
- [13] N. Takemura, S. Trebaol, M. Wouters, M. T. Portella-Oberli, and B. Deveaud, Polaritonic feshbach resonance, *Nature Physics* **10**, 500 (2014).
- [14] I. Bloch, J. Dalibard, and S. Nascimbène, Quantum simulations with ultracold quantum gases, *Nature Physics* **8**, 267 (2012).
- [15] I. M. Georgescu, S. Ashhab, and F. Nori, Quantum simulation, *Rev. Mod. Phys.* **86**, 153 (2014).
- [16] M. Leskinen, O. Nummi, F. Massel, and P. Törmä, Fermi-polaron-like effects in a one-dimensional (1d) optical lattice, *New Journal of Physics* **12**, 073044 (2010).
- [17] H. Hu, A.-B. Wang, S. Yi, and X.-J. Liu, Fermi polaron in a one-dimensional quasiperiodic optical lattice: The simplest many-body localization challenge, *Phys. Rev. A* **93**, 053601 (2016).
- [18] M. Bruderer, A. Klein, S. R. Clark, and D. Jaksch, Polaron physics in optical lattices, *Phys. Rev. A* **76**, 011605 (2007).
- [19] K. Keiler, S. I. Mistakidis, and P. Schmelcher, Doping a lattice-trapped bosonic species with impurities: From ground state properties to correlated tunneling dynamics, *New Journal of Physics* **22**, 083003 (2020).
- [20] G. Domínguez-Castro, Bose polaron in a one-dimensional lattice with power-law hopping, *Atoms* **11**, 110 (2023).

- [21] J.-H. Zeng, S. Yi, and L. He, Emergent mott insulators at noninteger fillings and devil's staircase induced by attractive interaction in many-body polarons, *Phys. Rev. A* **107**, 063309 (2023).
- [22] V. E. Colussi, F. Caleffi, C. Menotti, and A. Recati, Lattice polarons across the superfluid to mott insulator transition, *Phys. Rev. Lett.* **130**, 173002 (2023).
- [23] R. Alhyder and G. M. Bruun, Mobile impurity probing a two-dimensional superfluid phase transition, *Phys. Rev. A* **105**, 063303 (2022).
- [24] T. Fukuhara, A. Kantian, M. Endres, M. Cheneau, P. Schauß, S. Hild, D. Bellem, U. Schollwöck, T. Giamarchi, C. Gross, *et al.*, Quantum dynamics of a mobile spin impurity, *Nature Physics* **9**, 235 (2013).
- [25] F. Massel, A. Kantian, A. J. Daley, T. Giamarchi, and P. Törmä, Dynamics of an impurity in a one-dimensional lattice, *New Journal of Physics* **15**, 045018 (2013).
- [26] A. Privitera and W. Hofstetter, Polaronic slowing of fermionic impurities in lattice bose-fermi mixtures, *Phys. Rev. A* **82**, 063614 (2010).
- [27] M. Bruderer, A. Klein, S. R. Clark, and D. Jaksch, Transport of strong-coupling polarons in optical lattices, *New Journal of Physics* **10**, 033015 (2008).
- [28] A.-M. Visuri, T. Giamarchi, and P. Törmä, Excitations and impurity dynamics in a fermionic mott insulator with nearest-neighbor interactions, *Phys. Rev. B* **93**, 125110 (2016).
- [29] A.-M. Visuri, P. Törmä, and T. Giamarchi, Impurity and soliton dynamics in a fermi gas with nearest-neighbor interactions, *Phys. Rev. A* **95**, 063605 (2017).
- [30] A. Petković and Z. Ristivojevic, Mediated interaction between polarons in a one-dimensional bose gas, *Phys. Rev. A* **105**, L021303 (2022).
- [31] M. Pasek and G. Orso, Induced pairing of fermionic impurities in a one-dimensional strongly correlated bose gas, *Phys. Rev. B* **100**, 245419 (2019).
- [32] S. Dutta and E. J. Mueller, Variational study of polarons and bipolarons in a one-dimensional bose lattice gas in both the superfluid and the mott-insulator regimes, *Phys. Rev. A* **88**, 053601 (2013).
- [33] S. Ding, G. Domínguez-Castro, A. Julku, A. Camacho Guardian, and G. M. Bruun, Polarons and bipolarons in a two-dimensional square lattice, *SciPost Physics* **14**, 143 (2023).
- [34] V. R. Yordanov and F. Isaule, Mobile impurities interacting with a few one-dimensional lattice bosons, *Journal of Physics B: Atomic, Molecular and Optical Physics* **56**, 045301 (2023).
- [35] F. Isaule, A. Rojo-Francàs, and B. Juliá-Díaz, Bound impurities in a one-dimensional Bose lattice gas: Low-energy properties and quench-induced dynamics, *SciPost Phys. Core* **7**, 049 (2024).
- [36] M. Santiago-García and A. Camacho-Guardian, Collective excitations of a bose-einstein condensate of hard-core bosons and their mediated interactions: from two-body bound states to mediated superfluidity, *New Journal of Physics* **25**, 093032 (2023).
- [37] R. Paredes, G. Bruun, and A. Camacho-Guardian, Interactions mediated by atoms, photons, electrons, and excitons, *Phys. Rev. A* **110**, 030101 (2024).
- [38] L. A. P. Ardila, Ultra-dilute gas of polarons in a bose-einstein condensate, *Atoms* **10**, 10.3390/atoms10010029 (2022).
- [39] G. E. Astrakharchik, L. A. P. Ardila, K. Jachymski, and A. Negretti, Many-body bound states and induced interactions of charged impurities in a bosonic bath, *Nature Communications* **14**, 1647 (2023).
- [40] F. Gómez-Lozada, H. Hiyane, T. Busch, and T. Fogarty, Bose-fermi n -polaron state emergence from correlation-mediated blocking of phase separation (2024), [arXiv:2409.13785](https://arxiv.org/abs/2409.13785) [cond-mat.quant-gas].
- [41] A. Camacho-Guardian, N. Goldman, P. Massignan, and G. M. Bruun, Dropping an impurity into a chern insulator: A polaron view on topological matter, *Phys. Rev. B* **99**, 081105 (2019).
- [42] D. Pimenov, A. Camacho-Guardian, N. Goldman, P. Massignan, G. M. Bruun, and M. Goldstein, Topological transport of mobile impurities, *Phys. Rev. B* **103**, 245106 (2021).
- [43] F. Grusdt, N. Y. Yao, and E. A. Demler, Topological polarons, quasiparticle invariants, and their detection in one-dimensional symmetry-protected phases, *Phys. Rev. B* **100**, 075126 (2019).
- [44] A. Vashisht, I. Amelio, L. Vanderstraeten, G. M. Bruun, O. K. Diessel, and N. Goldman, Chiral polaron formation on the edge of topological quantum matter (2024), [arXiv:2407.19093](https://arxiv.org/abs/2407.19093) [cond-mat.quant-gas].
- [45] D. Pimenov, Polaron spectra and edge singularities for correlated flat bands, *Phys. Rev. B* **109**, 195153 (2024).
- [46] J. Koepsell, D. Bourgund, P. Sompet, S. Hirthe, A. Bohrdt, Y. Wang, F. Grusdt, E. Demler, G. Salomon, C. Gross, *et al.*, Microscopic evolution of doped mott insulators from polaronic metal to fermi liquid, *Science* **374**, 82 (2021).
- [47] J. Koepsell, J. Vijayan, P. Sompet, F. Grusdt, T. A. Hilker, E. Demler, G. Salomon, I. Bloch, and C. Gross, Imaging magnetic polarons in the doped fermi-hubbard model, *Nature* **572**, 358 (2019).
- [48] M. Lebrat, M. Xu, L. H. Kendrick, A. Kale, Y. Gang, P. Seetharaman, I. Morera, E. Khatami, E. Demler, and M. Greiner, Observation of nagaoka polarons in a fermi-hubbard quantum simulator, *Nature* **629**, 317 (2024).
- [49] P. Weckesser, K. Srakaew, T. Blatz, D. Wei, D. Adler, S. Agrawal, A. Bohrdt, I. Bloch, and J. Zeiher, Realization of a rydberg-dressed extended bose hubbard model (2024), [arXiv:2405.20128](https://arxiv.org/abs/2405.20128) [cond-mat.quant-gas].
- [50] S. Baier, M. J. Mark, D. Petter, K. Aikawa, L. Chomaz, Z. Cai, M. Baranov, P. Zoller, and F. Ferlaino, Extended bose-hubbard models with ultracold magnetic atoms, *Science* **352**, 201 (2016).
- [51] B. Yan, S. A. Moses, B. Gadway, J. P. Covey, K. R. Hazzard, A. M. Rey, D. S. Jin, and J. Ye, Observation of dipolar spin-exchange interactions with lattice-confined polar molecules, *Nature* **501**, 521 (2013).
- [52] J.-R. Li, K. Matsuda, C. Miller, A. N. Carroll, W. G. Tobias, J. S. Higgins, and J. Ye, Tunable itinerant spin dynamics with polar molecules, *Nature* **614**, 70 (2023).
- [53] F. J. Burnell, M. M. Parish, N. R. Cooper, and S. L. Sondhi, Devil's staircases and supersolids in a one-dimensional dipolar bose gas, *Phys. Rev. B* **80**, 174519 (2009).
- [54] H. Korbmayer, G. A. Domínguez-Castro, W.-H. Li, J. Zakrzewski, and L. Santos, Transversal effects on the ground state of hard-core dipolar bosons in one-dimensional optical lattices, *Phys. Rev. A* **107**, 063307 (2023).

- [55] I. Amelio and N. Goldman, Polaron spectroscopy of interacting Fermi systems: Insights from exact diagonalization, *SciPost Phys.* **16**, 056 (2024).
- [56] I. Amelio, G. Mazza, and N. Goldman, Polaron formation in insulators and the key role of hole scattering processes: Band insulators, charge density waves and mott transition (2024), [arXiv:2408.01377](https://arxiv.org/abs/2408.01377) [cond-mat.str-el].
- [57] T. Smoleński, P. E. Dolgirev, C. Kuhlenkamp, A. Popert, Y. Shimazaki, P. Back, X. Lu, M. Kroner, K. Watanabe, T. Taniguchi, et al., Signatures of wigner crystal of electrons in a monolayer semiconductor, *Nature* **595**, 53 (2021).
- [58] Y. Shimazaki, C. Kuhlenkamp, I. Schwartz, T. Smoleński, K. Watanabe, T. Taniguchi, M. Kroner, R. Schmidt, M. Knap, and A. m. c. Imamoğlu, Optical signatures of periodic charge distribution in a mott-like correlated insulator state, *Phys. Rev. X* **11**, 021027 (2021).
- [59] G. Mazza and A. Amaricci, Strongly correlated exciton-polarons in twisted homobilayer heterostructures, *Phys. Rev. B* **106**, L241104 (2022).
- [60] A. Go and G. S. Jeon, Phase transitions and spectral properties of the ionic hubbard model in one dimension, *Phys. Rev. B* **84**, 195102 (2011).
- [61] J. De Marco, L. Tolle, C.-M. Halati, A. Sheikhan, A. M. Läuchli, and C. Kollath, Level statistics of the one-dimensional ionic hubbard model, *Phys. Rev. Res.* **4**, 033119 (2022).
- [62] M. Sekania, D. Baeriswyl, L. Jibuti, and G. I. Japaridze, Mass-imbalanced ionic hubbard chain, *Phys. Rev. B* **96**, 035116 (2017).
- [63] C. D. Batista and A. A. Aligia, Exact bond ordered ground state for the transition between the band and the mott insulator, *Phys. Rev. Lett.* **92**, 246405 (2004).
- [64] T. Wilkens and R. M. Martin, Quantum monte carlo study of the one-dimensional ionic hubbard model, *Phys. Rev. B* **63**, 235108 (2001).
- [65] J. Hauschild and F. Pollmann, Efficient numerical simulations with Tensor Networks: Tensor Network Python (TeNPy), *SciPost Phys. Lect. Notes* , 5 (2018).
- [66] T. Giamarchi, *Quantum physics in one dimension*, Vol. 121 (Clarendon press, 2003).
- [67] M. Santiago Garcia, S. Castillo Lopez, and A. Camacho, Lattice polaron in a bose-einstein condensate of hard-core bosons, *New Journal of Physics* **10.1088/1367-2630/ad503e** (2024).
- [68] J. Hubbard and J. B. Torrance, Model of the neutral-ionic phase transformation, *Phys. Rev. Lett.* **47**, 1750 (1981).
- [69] P. J. Strebler and Z. G. Soos, Theory of charge transfer in aromatic donor-acceptor crystals, *The Journal of Chemical Physics* **53**, 4077 (1970).
- [70] N. Nagaosa and J.-i. Takimoto, Theory of neutral-ionic transition in organic crystals. i. monte carlo simulation of modified hubbard model, *Journal of the Physical Society of Japan* **55**, 2735 (1986).
- [71] N. Nagaosa and J.-i. Takimoto, Theory of neutral-ionic transition in organic crystals. ii. effect of the intersite coulomb interaction, *Journal of the Physical Society of Japan* **55**, 2745 (1986).
- [72] T. Egami, S. Ishihara, and M. Tachiki, Lattice effect of strong electron correlation: Implication for ferroelectricity and superconductivity, *Science* **261**, 1307 (1993).
- [73] M. Fabrizio, A. O. Gogolin, and A. A. Nersesyan, From band insulator to mott insulator in one dimension, *Phys. Rev. Lett.* **83**, 2014 (1999).
- [74] L. A. Peña Ardila, M. Heyl, and A. Eckardt, Measuring the single-particle density matrix for fermions and hard-core bosons in an optical lattice, *Phys. Rev. Lett.* **121**, 260401 (2018).
- [75] A. Camacho-Guardian, L. A. Peña Ardila, T. Pohl, and G. M. Bruun, Bipolarons in a bose-einstein condensate, *Phys. Rev. Lett.* **121**, 013401 (2018).
- [76] M. Will, G. E. Astrakharchik, and M. Fleischhauer, Polaron interactions and bipolarons in one-dimensional bose gases in the strong coupling regime, *Phys. Rev. Lett.* **127**, 103401 (2021).